Desalination and Water Treatment
www.deswater.com
doi: 10.5004/dwt.2023.29664

298 (2023) 117–126
June

Synthesis and characterization of iron-doped titania nanoparticles for the removal of DPP-IV inhibitor from the aqueous samples

Muhammad Irfan Jalees[a,*], Yousara Rauf[a], Arfa Iqbal[a], Nayab Zahara[a], Emre Cevik[b]

[a]*Institute of Environmental Engineering and Research, University of Engineering and Technology, Lahore, Pakistan, 54890, emails: irfan611@gmail.com (M.I. Jalees) ORCID: 0000-0003-3762-3124, yousararauf123@gmail.com (Y. Rauf), arfa.libra@gmail.com (A. Iqbal), nayab_zahara2009@hotmail.com (N. Zahara)*
[b]*Bioenergy Research Unit, Department of Biophysics, Institute for Research and Medical Consultations, Imam Abdulrahman Bin Faisal University, 1982, P.O. Box: 1982, Dammam 31441, Saudi Arabia, email: ecevik@iau.edu.sa*

Received 21 September 2022; Accepted 30 May 2023

ABSTRACT

Human excretion contains metabolites, when entering the drinking water stream, can cause a lowering of blood pressure, arterial inflammation, neointima formation, etc. Various types of medicines are consumed by the patient. These medicines, through excretion, enter the ecosystem. Being persistent, these medicines remain in the ecosystem and can cause chronic effects on the fauna and flora of any ecosystem. Many treatment methods, that is, coagulation, advanced oxidation, and adsorption were proposed for these medicines but due to cost and sludge production, the results are not favorable. In this study novel, iron-titania nanoparticles were synthesized for the treatment of sitagliptin which is diabetic II medicine (DPP-IV). Characteristics peaks X-ray diffraction at 27.52°, 33.39°, 35.65°, and 53.26° indicated the crystalline structure while scanning electron microscopy/energy-dispersive X-ray spectroscopy confirmed the required molar ratio of iron and titania with a size of 100–290 nm. The method validation results for sitagliptin showed 0.69 RSD%, 34 ppm limit of quantification, and 11 ppm limit of detection. Optimization of parameters was performed using Taguchi design of experiment which gave 80% removal efficiency of sitagliptin at 7 pH, 10 min, 200 mg of dose, and 70 ppm concentration. The adsorption isotherms models suggested a multilayer process (Freundlich isotherm), with an adsorption energy of –8.6 kJ/mol (exothermic and spontaneous). Kinetic studies indicated that the adsorption process followed second-order kinetics.

Keywords: Iron; Titania; Nanoparticles; DDP-IV inhibitor; Sitagliptin

1. Introduction

The increasing water demand due to the increased global population leads to scarcity of water on a large scale. Inadequate sanitation, the continuous emergence of waterborne diseases, and the disruption of water quality are the major factors responsible for the deterioration of existing water bodies [1]. Out of many, pharmaceutical chemicals are one of the pollutants which have adverse effects on waste bodies. These compounds are present in the range of ng/L to μg/L in the wastewater stream even though these minor quantities are posing serious impacts on the environment [2,3]. The major components of pharmaceuticals are antibiotics, antihistamines, steroids, anticancer, etc. These pharmaceuticals have a very low bioaccumulation rate of 20%–30% in humans and animals [4]. To maintain a healthy life, medicines are used that are potent for the human body and animals after excretion from the body. Human and animal excretions (in the form of wastewater) are discharged in lakes and rivers in the form of metabolites.

* Corresponding author.

1944-3994/1944-3986 © 2023 Desalination Publications. All rights reserved.

These metabolites, persistent in nature, are posing chronic effects on both flora and fauna.

Among many, sitagliptin which is a DDP-IV inhibitor was studied using nanoparticles in this research. Sitagliptin is one of the dipeptidyl peptidase-4 inhibitors, also called DPP-4 inhibitors, which are classified as novel oral antihyperglycemic agents and are commonly used to treat type 2 diabetes mellitus [5]. Sitagliptin is well absorbed orally and has a bioavailability of 87%. The suggested dose for sitagliptin may vary from 25 to 100 mg once a day for 30 weeks depending on the condition [6]. An amount of 3.25–13 mg of sitagliptin excreted from the human body has a half-life 12.8 h based on the consumption and excretion rate, the predicted environmental concentration was calculated using Eq. (1) given by the Technical Guidance Document of the European Commission on Risk Assessment [7]. The obtained value was 1.974×10^{-5} mg/L.

$$\mathrm{PEC}_{\left(\frac{g}{L}\right)} = \frac{A \times \left(\frac{1-R}{100}\right)}{365 \times P \times V \times 100} \tag{1}$$

where A (kg): total medicine utilized every year in a country; R (%): elimination rate; P: number of inhabitants in a country; V (m^3): amount of wastewater per inhabitant per day.

This sitagliptin deposited in aquatic animals and plants, if consumed by humans, may have significant effects like lowering blood pressure, arterial inflammation, neointima formation, circulating endothelial progenitor cells, and increased homeostasis [8,9]. Hence, the treatment of sitagliptin was required.

Many researchers are now working on the treatment of these persistent compounds. They used different techniques for the treatment of water that includes biofilms [10], ultrasound-persulphate [11], catalytic ozonation [12], microbubble ozonation [13], microalgae [14], and electrocoagulation [15]. Production of secondary hazardous and toxic pollutants, consumption of a large amount of energy, and production of sludge minimize the efficiency of these mentioned methods. Researchers are now moving for the adsorption process through nanoparticles [16] as adsorbents due to their high thermal stability, high porosity, and high surface area [17]. Different types of metal nanoparticles like TiO_2, ZnS, ZnO, CdS, Fe_2O_3 [18], PES/silica nanoparticles [19], Ni/graphene nanoparticles [20], PVC/PC/MAg membrane [21], and Cu/Ag nanocomposite [22], etc. have been reported as very effective in the degradation of pharmaceuticals.

Recently, it has been investigated that introducing one or two metals onto the TiO_2 nanoparticles, can improve the removal efficiency of nanoparticles against the removal of different pharmaceuticals. Thus, co-doping of different materials like metallic or non-metallic ions may produce a synergetic impact to enhance the potential of TiO_2 nanoparticles against the removal of pharmaceutical compounds [23]. In one study, 94% degradation of amoxicillin was observed by using Co-doped TiO_2 nanoparticles [24], whereas, in another study, Cu-TiO_2 nanoparticles were evaluated against the removal of naproxen and 87% removal was observed [25]. One other study shows the complete removal of bisphenol A by using Zr-TiO_2 nanoparticles [26].

Considering all the above aspects, in this study novel, iron doped-titania nanoparticles were synthesized and characterized using Fourier-transform infrared spectroscopy, X-ray diffraction (XRD), scanning electron microscopy (SEM), and energy-dispersive X-ray spectroscopy (EDX). The synthesized nanoparticles were used for the first time in the treatment of sitagliptin in an aqueous solution using the LxL^4 design of the experiment (Taguchi). To study the tentative mechanism different mathematical isotherm models were also studied.

2. Materials and methods

2.1. Synthesis of iron-doped titania nanoparticles

The nanoparticles were prepared by the co-precipitation method [27]. Titania (5.79g, Merck, Pakistan) was added to 21 mL of ethanol (Merck, Pakistan) and stirred (700 rpm) at room temperature for 2 h. Afterwards, 8 mL of distilled water and 7.84 g of $FeCl_3 \cdot 6H_2O$ (Merck, Pakistan) were added and further stirred for 2 h. The resultant slurry was placed in the oven at 100°C till the color changed to light yellow. This was further transferred to a furnace at 550°C for drying. The dried product was kept in an airtight jar and used when required.

2.2. Analytical analysis

The prepared nanoparticles were analyzed using XRD (Bruker 2D Phaser, MA, USA) having Cu-Kα at 0.154178 nm (λ). The θ range was 20°–60° and the voltage was 30 kV with 10 mA. The size of the nanoparticles was analyzed using Litesizer 500® in ethanol (as solvent). The morphology was studied using SEM with EDX and E-beam lithograph (FEI Nova 450 NanoSEM, Thermo Fisher, MA, USA). The operating conditions of SEM/EDX were 10 kV (HV), 3 (spot size), 0.1 μS (dwell time), ETD (detector), and 4 frames (filtering). The results of XRD and SEM/EDX are given in Fig. 2.

2.3. Method validation

For analysis of the sitagliptin method validation on a UV-Visible spectrophotometer was performed. For this purpose, a standard solution of 1,000 ppm in distilled water was prepared. This stock solution was used to prepare standard solutions from 50–80 ppm. The standard solutions were analyzed on a UV-Visible spectrophotometer at 267 nm. The calibration curve of it is shown in Fig. 1. The various parameters calculated based on this calibration for method validation are given in Table 1. Various parameters like linearity, precision, the limit of detection (LOD), and the limit of quantification (LOQ) were calculated (Table 1).

The following equations were for LOD and LOQ.

$$\mathrm{LOD} = \frac{3.3 \times \mathrm{SD\,of\,Intercept}}{\mathrm{Slope}} \tag{2}$$

$$\mathrm{LOQ} = \frac{10 \times \mathrm{SD\,of\,Intercept}}{\mathrm{Slope}} \tag{3}$$

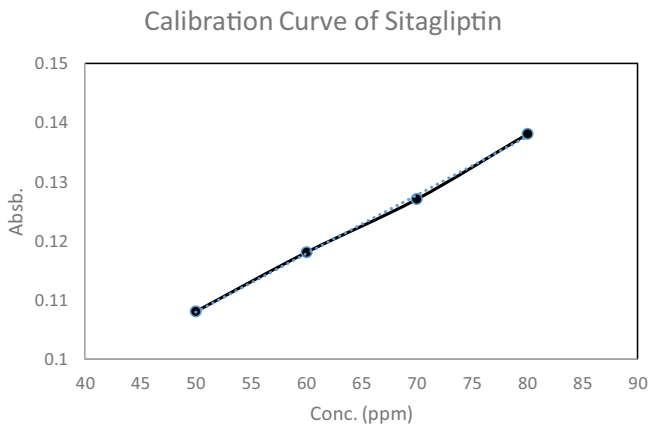

Fig. 1. Calibration curve of standard sitagliptin solution at 267 nm wavelength.

2.4. Taguchi design of experiment (DOE) for optimization of parameters

The optimization of parameters was performed based on the initial concentration of sitagliptin, adsorbent dose, pH, and contact time. Taguchi's design of the experiment (DOE) was to define various values of optimized parameters. A set of 16 experiments were performed using the LxL (16) design of Taguchi. Table 2 has the list of experiments that were performed in the optimization of parameters. The experimentation was carried out in triplicate and contained blank samples and control samples. The results have a standard deviation of 0.63.

2.5. Isotherms and kinetic study

At optimized conditions, different isotherms and kinetic models were studied. The different mathematical models for this purpose are given in Table 3.

3. Results and discussions

3.1. Characterization of iron-doped titania nanoparticles

Nanoparticles were characterized using XRD, SEM, and EDX (Fig. 2). In the case of XRD, different peaks were observed at 2θ values of 24.14°, 33.15°, 35.61°, 35.9°, 41.71°, 49.48°, and 54.09° with inter planer spaces of 012, 104, 110, 111, 200, 024, and 116. The d spacing values were in the range of 4.3–5.0 Å. The crystalline structure of the nanoparticle is hexagonal, $R\bar{3}c$, (167), $Z = 6$. The results are characteristic of iron-titania nanoparticles [28,29]. The particle size analysis (Fig. 2) indicated that the synthetic nanoparticles were in the range of 280–630 nm. The SEM analysis of the nanoparticles showed the presence of agglomerates and clusters. EDX analysis showed the successful formation of iron-titania nanoparticles as the analysis showed the presence of Fe and TiO in the samples. The weight % of "Fe" was 5.6 while for "Ti" it was 10.5 (Fig. 2).

3.2. Optimization of parameters

The removal of sitagliptin was evaluated by varying the parameters, that is, contact time, dose, concentration, and pH as per Taguchi's design of experiment. The removal efficiency was calculated using Eq. (4).

Table 1
Results of method validation of sitagliptin in distilled water using UV-Visible spectrophotometer in this study

Conc. (ppm)	Absorbance	Found conc.	Recovery (%)
50	0.11	49.6	99.2
60	0.12	59.6	99.3
70	0.13	68.6	98.0
80	0.14	79.6	99.5
Parameter			
Mean	99.008		
St. dev.	0.683		
SE of intercept	0.002		
SD of intercept	0.003		
Limit of detection	11.517		
Limit of quantification	34.900		
R	0.999		
RSD%	0.690		
Slope	0.001		
Intercept	0.058		
R^2	0.999		

Table 2
Set of experiments showing the values of different parameters for the batch adsorption studies for the removal of sitagliptin using nanoparticles

Sr.	Conc. (ppm)	pH	Dose (mg)	Time (min)	RE %
1.	50	3	50	10	62.54
2.	50	5	100	20	25.14
3.	50	7	150	30	89.19
4.	50	9	200	40	90.7
5.	60	3	100	30	62.33
6.	60	5	50	40	66.09
7.	60	7	200	10	74.85
8.	60	9	150	20	13.72
9.	70	3	150	40	59.58
10.	70	5	200	30	77.05
11.	70	7	50	20	63.89
12.	70	9	100	10	95.11
13.	80	3	200	20	90.16
14.	80	5	150	10	82.71
15.	80	7	100	40	65.46
16.	80	9	50	30	49.78

$$\text{Removal Efficiency}(\%) = \frac{\text{Initial Concentration} - \text{Final Concentration}}{\text{Initial Concentration}} \times 100 \quad (4)$$

Table 3
Mathematical model calculations using different isotherms for the removal of sitagliptin from aqueous solution using iron-titania nanoparticles

Model name	Mathematical form	Parameters	Values
Langmuir	$\frac{C_e}{q_e}=\frac{1}{bQ_{\max}}+\frac{C_e}{Q_{\max}}$ (5)	$Q_{\max}$	0.06 mg/g
		b	1.39 L/mg
		R_L	0.014
		R^2	0.99
Freundlich	$\log q_e=\log K_f+\frac{1}{n}\log C_e$ (6)	n	0.39
		K_f	12.9 mg/g
		R^2	0.99
Temkin	$q_e=\frac{RT}{b_T}\ln A_T+\frac{RT}{b_T}\ln C_e$ (7)	A	0.68
		B	10.03
		R^2	0.84
Dubinin–Radushkevich	$\log\left(\frac{\theta}{C_o}\right)=\log\left(K_{\text{fh}}\right)+n\log\left(1-\theta\right)$ (8)	K_{ad}	80.00
		$Q_{\max}$	4.42 mg/g
		E	0.08
		R^2	0.96
Flory–Huggins	$\log\frac{\theta}{C_o}=\log K_{\text{FH}}+n\log\left(1-\theta\right)$ (9)	n	0.98
		K_{FH}	219.01 L/mol
		ΔG	–8.67 kJ/mol
		R^2	0.98
Pseudo-first-order	$\log\left(q_e-q_t\right)=\log q_e-\frac{k_1}{2.303}t$ (10)	q_e	2.2297 mg/g
		k_1	–0.0152 min
		R^2	0.8763
Pseudo-second-order	$\frac{t}{q_t}=\frac{1}{k_2q_e^2}+\frac{1}{q_e}t$ (11)	q_e	166.6 mg/g
		k_2	3.14×10^{-6} g/mg·min
		R^2	0.933

Eq. (5): C_e: Equilibrium concentration of adsorbate (mg/L); q_e: the amount of metal adsorbed per gram of adsorbate at equilibrium; q_m: maximum monolayer coverage capacity (mg/g); b: Langmuir isotherm constant.
Eq. (6): K_f: Freundlich isotherm constant; n: adsorption intensity.
Eq. (7): β: Temkin constant.
Eq. (8): q_s: Theoretical isotherm saturation capacity; K_{ad}: Dubinin–Radushkevich isotherm constant; ε: Dubinin–Radushkevich.
Eq. (9): θ: degree of surface coverage; n: number of ions occupying adsorption sites; K_{FH}: Flory–Huggins isotherm constant.

The RE % ranged from 25% to 95% (Table 2). At 10 min and 7 pH, the maximum RE % indicated that the adsorption process was not affected by hydrogen and hydroxyl ions. Maximum adsorption sites were available at a dose of 200 mg of adsorbent which resulted in good RE %. A maximum of 70 ppm dose of sitagliptin gave good RE % as per the given dose active sites. The mean plots of adsorption parameters are shown in Fig. 3. The highest RE % was obtained between 50–200 mg/L of dose which indicated that the adsorbent dose is the most important parameter affecting the removal efficiency. Afterward, contact time is the second most affecting parameter for the removal efficiency giving a removal efficiency of more than 75%. Based on the results obtained for RE %, contour plots were drawn to discuss the interaction between variable and their effects on sitagliptin removal. Fig. 4 illustrates the influence of different parameters on the removal of sitagliptin. In the case of pH vs. time, by increasing the pH between 6–8 and contact time between 35–40 min, RE % was more than 80%. The longer contact time allows pollutants to occupy all the available adsorption sites on the surface of the adsorbent [6]. The adsorbent dose vs time indicated that increasing the dose from 150 to 200 mg/L increases the surface area (active sites) and more adsorption tools placed which increases the RE %. The initial concentration of sitagliptin (<65 ppm) showed very little RE % because of the low interaction energy and contact time available for the process [30]. The effects of dose and initial concentration showed that by increasing the concentration and dose RE % increased which was a known trend due to the abundance of active site availability [1]. The extreme contour gradient shows that the adsorption process was purely based on the available surface area [31]. The elliptical contour plots also depict that the adsorption process was very rapid at the start, and it declines towards higher doses which leads to higher turbidity in the solution. This turbidity requires additional treatment and increases the operational cost.

3.3. Adsorption isotherms modeling

Five adsorption isotherms Langmuir, Freundlich, Temkin, Dubinin–Radushkevich, and Flory–Huggins were studied for the removal (a tentative mechanism) of

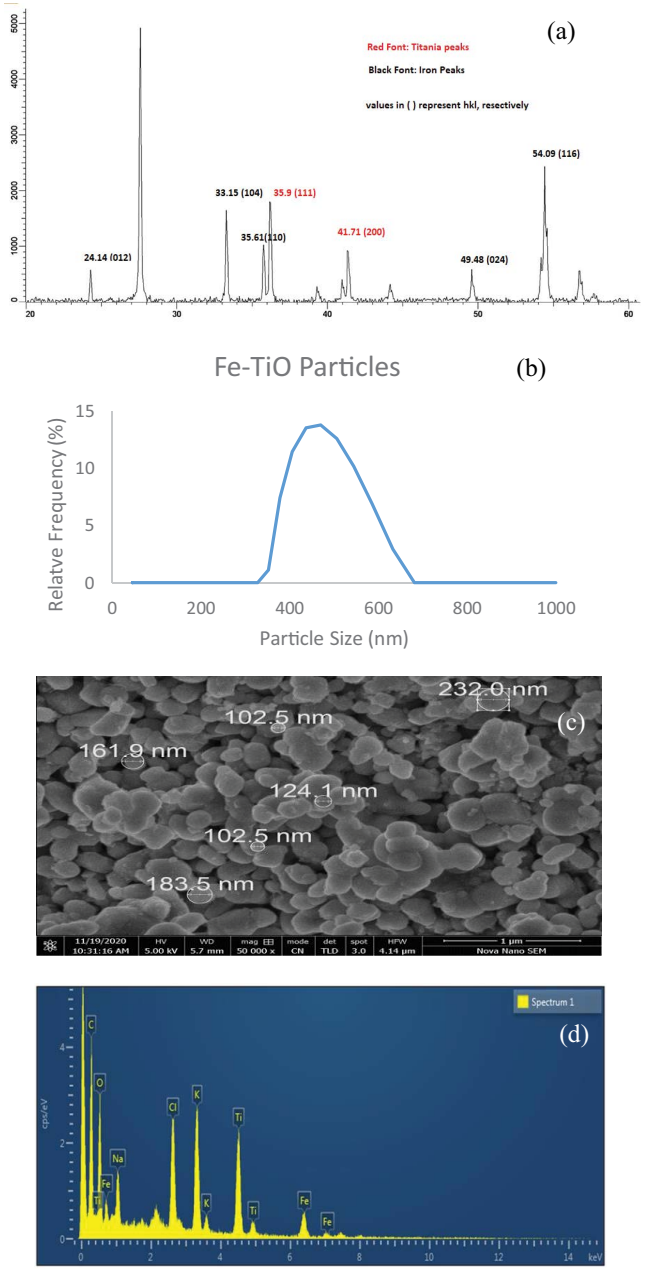

Fig. 2. Results of characterization of iron-titania nanoparticles using (a) X-ray diffraction, (b) particle size, (c) scanning electron microscopy, (d) energy-dispersive X-ray spectroscopy showing the successful formation of nanoparticles.

sitagliptin using iron-titania nanoparticles. The isotherms plots are illustrated in Fig. 5. The concentration of sitagliptin varied from 20–80 ppm at 7 pH, 10 min, and 200 mg/L dose of adsorbent. The mathematical model of isotherms is given in Table 3. Langmuir plot between logC_e and C_e/q_e, where C_e is the concentration of sitagliptin at equilibrium, while q_e is the experimental adsorption capacity. The results indicate that the monolayer adsorption with maximum adsorption (>90%) capacity at 200 mg of the adsorbent dose. The constant b was 1.39 and R_L was 0.1 which indicates that the nanoparticles have good affinity for the

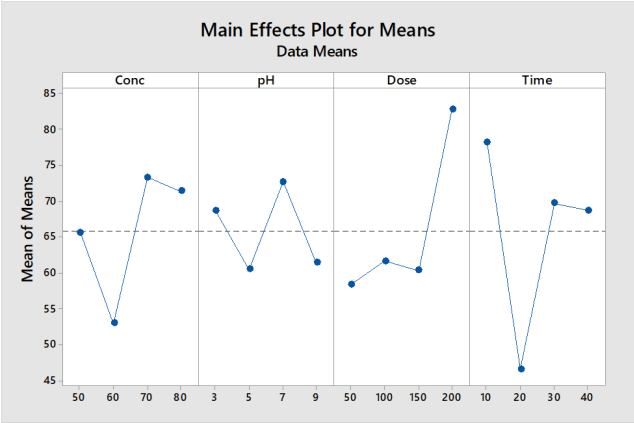

Fig. 3. Mean plots of various adsorption parameters showing the effect on removal efficiency of sitagliptin using nanoparticles.

sitagliptin which makes adsorption a favorable process [32]. Freundlich isotherm plot was drawn between logC_e and logq_e. The K_f (adsorption capacity) and n (adsorption intensity) were 12.93 mg/g and 0.38, respectively. This indicated that the adsorption process was multilayer [32]. As the R^2 value Freundlich isotherm is higher than the Langmuir therefore it suggested that the Freundlich model was more suited than Langmuir for sitagliptin removal [33]. Temkin isotherm explains adsorption energy and adsorbate–adsorbent interaction. The constants A (binding constant) and B (binding energy) were 0.68 and 10.31, respectively. This suggested that the process of adsorption was exothermic [34]. The high value of the correlation coefficient indicated that the adsorption process was chemisorption with physical attraction [32]. Dubinin–Radushkevich explains the porosity of the adsorbent. The constant Q_{max} (maximum theoretical isotherm saturation capacity), K_{ad} (Dubinin–Radushkevich constant), and E (mean adsorption energy) were 4.42 mg/g, 80, and 0.08, respectively. These results supported the chemisorption adsorption with dominant physical attraction as the value of E is less than 8 kJ/mol [1,32]. Flory–Huggins isotherms explain the degree of surface coverage of adsorption sites on the surface of the adsorbent. The constant n (number of ions occupying adsorbent sites) and ΔG (Gibbs free energy) was 0.98 and –8.67 kJ/mol, respectively. This indicated that nanoparticles have enough adsorption active sites where sitagliptin can adsorbed spontaneously (Table 3). Overall, the adsorption process was multilayer, spontaneous, and exothermic in nature. The tentative mechanism of the adsorption is given in Fig. 6.

3.4. Kinetics adsorption model

To study the kinetics (pseudo-first-order and pseudo-second-order), plots between t vs. log($q_e - q_t$) and t/q_t vs. t were used (Fig. 7). The value for the correlation coefficient for pseudo-second-order was closer to 1, that is, (R^2 = 0.93) than first-order which was 0.87 which indicated that the adsorption process was chemisorption as mentioned in the literature [35,36]. Furthermore, the values of experimental and theoretical adsorption capacity for pseudo-second-order was minimal which supported the pseudo-second-

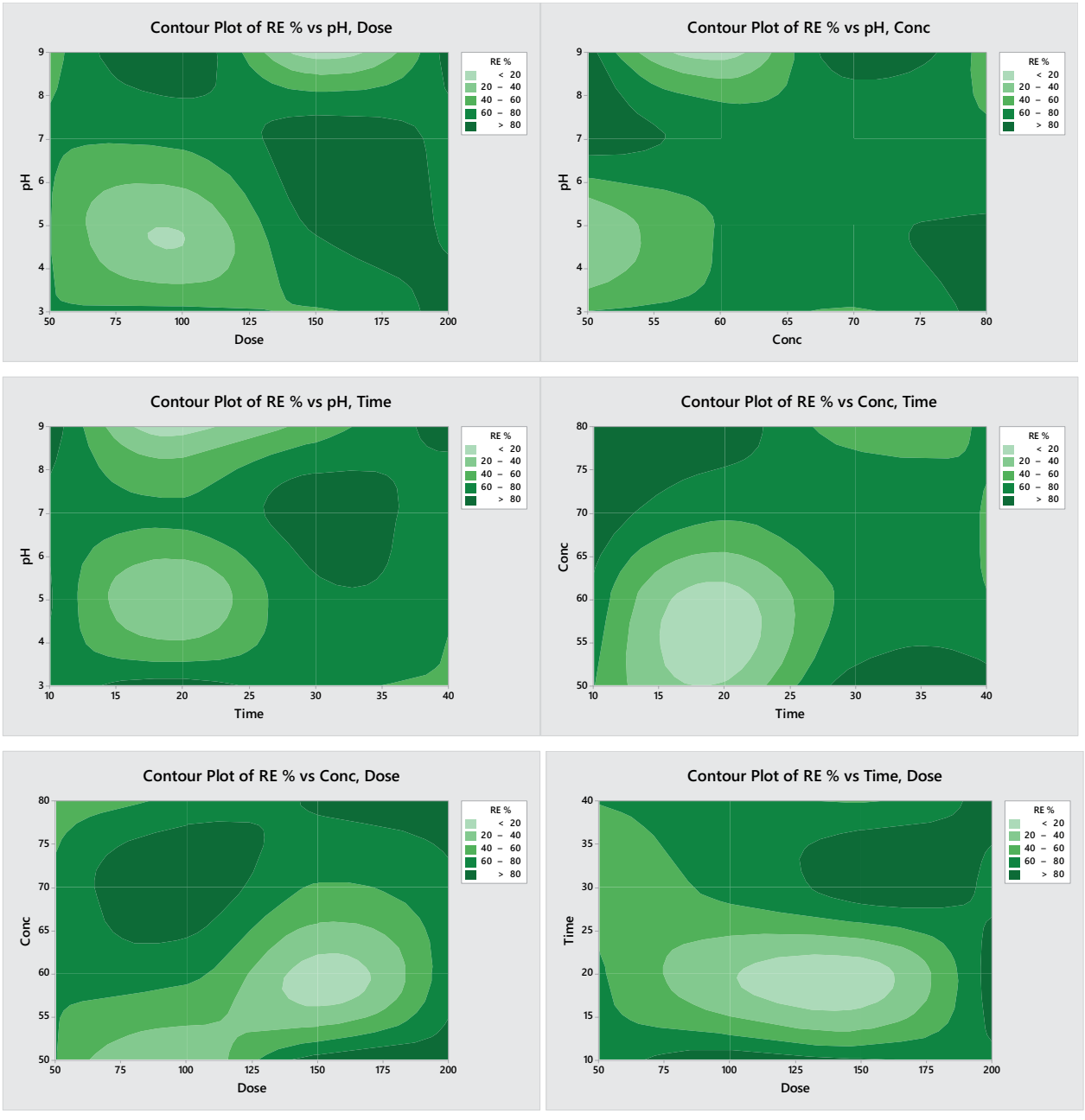

Fig. 4. Contour plots of various adsorption parameters for the removal of sitagliptin from an aqueous solution using iron-titania nanoparticles.

order kinetics in adsorption [37]. When the outer side of the nanoparticles is filled with the components of sitagliptin present in the wastewater, it starts entering the pores of the adsorbent available for the process. The fast adsorption kinetics increases the efficiency and reliability of the adsorbent [1]. The removal process reaches equilibrium in 10 min (Table 1).

Table 4 demonstrates that the removal efficiency of iron-doped titania nanoparticles towards the removal of the understudied pollutant was found extraordinarily superior to different materials of doped titania adsorbents (reported in the literature), which were investigated for the removal of various pharmaceutical drugs from water. The researcher used different nanoparticles for the removal of persistent pollutants from wastewater but have a less removal efficiency than the under-study nanoparticles hence making the use of these nanoparticles superior to other literature reported studies.

3.5. Cost analysis

The cost analysis of the synthetic nanoparticles is summarized below. A $0.38 is required for the treatment of 1 L of water containing sitagliptin as a pollutant.

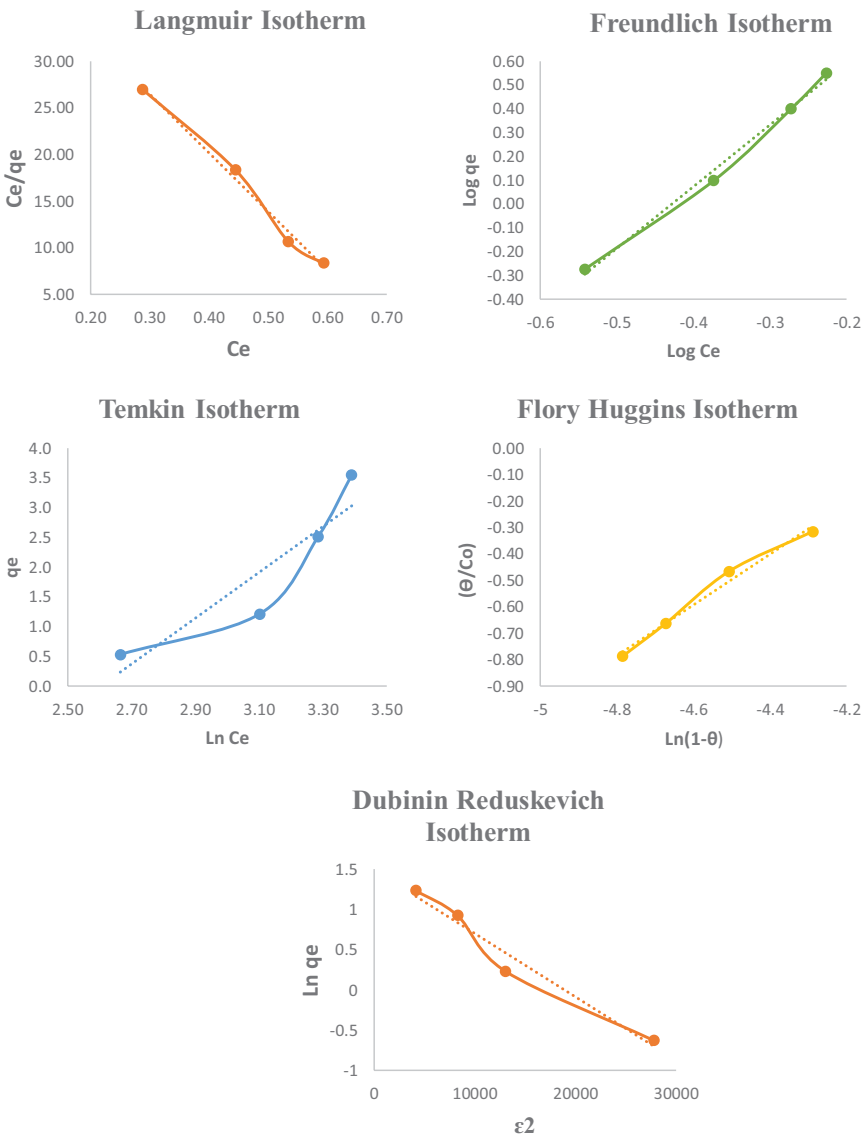

Fig. 5. Result of various isotherm plots obtained for the removal of sitagliptin using iron-nanoparticles at 7 pH, 200 mg/L dose, and 10 min contact time.

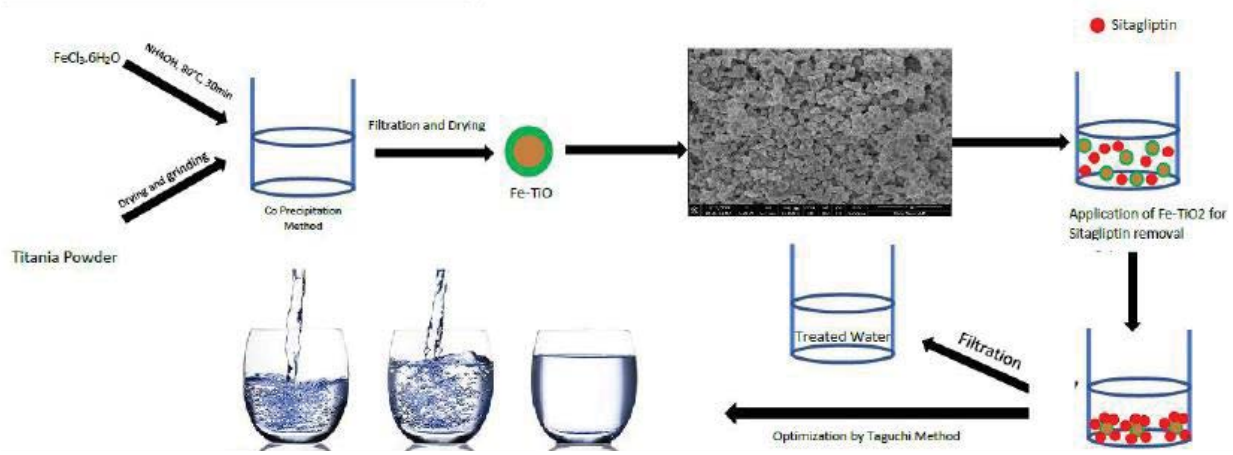

Fig. 6. Schematic diagram for the removal of sitagliptin from the sample solution.

Cost of titania	$0.026/1 g
Cost of $FeCl_3 \cdot 6H_2O$	$0.28/1 kg
Cost of ethanol	$1.5/1
Cost of nanoparticles (titania + iron salt + ethanol + electricity charges)	0.342 + 0.0024 + 0.0315 + 0.01 = $0.3859
Cost of treatment	$0.3859 L

Table 4
Comparison of pollutant removal efficiencies of nano adsorbents (reported in the literature) with present research

Different materials used	Pollutant removal	Removal efficiency (%)	References
Fe-TiO_2	Sitagliptin (DPP-IV)	80	Present study
Agro waste-TiO_2	Sulfamethoxazole	50	[38]
N/S-TiO_2	Diclofenac	70	[39]
B-TiO_2	Metoprolol	70	[40]
Zn-TiO_2	Ciprofloxacin	28.75	[41]
Ag-TiO_2	Amoxicillin	63.48	[42]
Fe^{3+}-$TiO_{2-x}N_x$	Diclofenac	72.3	[24]

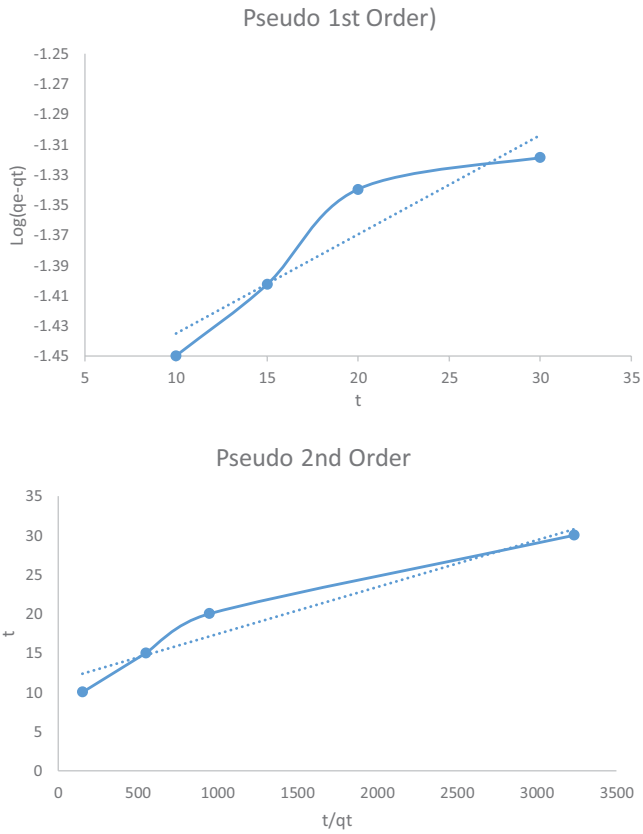

Fig. 7. Response of pseudo kinetics for the removal of sitagliptin using iron-titania nanoparticles.

4. Conclusion

In this study, the iron-doped titania nanoparticles are synthesized and characterized by XRD, SEM, and EDX. The results indicated the successful formation of nanoparticles. These nanoparticles were used for the removal of sitagliptin. The UV-Visible spectrophotometer was used for the method validation for sitagliptin. The result showed that the method was precise, and accurate and had LOD (11.5 ppm) and LOQ (34.9 ppm). Taguchi's design experiment suggested 16 sets of experiments that gave more than 80% removal efficiency under batch adsorption studies. The maximum adsorption capacity of iron-titania nanoparticles was 4.42 mg/g for sitagliptin. The optimized parameter values were contact time (10 min), pH (7), initial concentration (70 ppm), and adsorbent dose (200 mg/L). The adsorption isotherms model suggested that the adsorption process was multilayer chemisorption, exothermic and spontaneous. Kinetic studies indicated that the adsorption process followed second-order kinetics. Overall, the nanoparticles are novel and gave exceptionally reliable results for batch experiments for the removal of sitagliptin and can be used in continuous studies for future research.

Statements and declarations

Ethics approval and consent to participate

Not applicable.

Consent for publication

Not applicable.

Availability of data and materials

Can be provided on request.

Competing interests

Authors have no competing interest whatsoever.

Funding

Not applicable.

Authors' contributions

Muhammad Irfan Jalees: Original Idea and manuscript writing; Yousara Rauf: Experimental, result compilation, initial draft; Arfa Iqbal: Experimental; Nayab Zahara: Experimental; Emre Cevik: Manuscript review.

Acknowledgment

The authors are thankful to the University of Engineering and Technology, Lahore for providing the necessary facilities for study.

References

[1] M.I. Jalees, Synthesis and application of magnetized nanoparticles to remove lead from drinking water: Taguchi design of experiment, J. Water Sanit. Hyg. Dev., 10 (2020) 56–65.
[2] W.C. Li, Q.G. Niu, H. Zhang, Z. Tian, Y. Zhang, Y.X. Gao, Y.-Y. Li, O. Nishimura, M. Yang, UASB treatment of chemical synthesis-based pharmaceutical wastewater containing rich organic sulfur compounds and sulfate and associated microbial characteristics, Chem. Eng. J., 260 (2015) 55–63.
[3] D. Kanakaraju, B.D. Glass, M. Oelgemöller, Titanium dioxide photocatalysis for pharmaceutical wastewater treatment, Environ. Chem. Lett., 12 (2014) 27–47.
[4] M. Ahmadi, H.R. Motlagh, N. Jaafarzadeh, A. Mostoufi, R. Saeedi, G. Barzegar, S. Jorfi, Enhanced photocatalytic degradation of tetracycline and real pharmaceutical wastewater using MWCNT/TiO_2 nano-composite, J. Environ. Manage., 186 (2017) 55–63.
[5] K.-F. Liao, C.-L. Lin, S.-W. Lai, W.-C. Chen, Sitagliptin use and risk of acute pancreatitis in type 2 diabetes mellitus: a population-based case-control study in Taiwan, Eur. J. Intern. Med., 27 (2016) 76–79.
[6] C. Ballav, S.C.L. Gough, Safety and efficacy of sitagliptin-metformin in fixed combination for the treatment of type 2 diabetes mellitus, Clin. Med. Insights: Endocrinol. Diabetes, 6 (2013) 25–37.
[7] T.M.S. Attia, X.L. Hu, Y.D. Qiang, Synthesized magnetic nanoparticles coated zeolite for the adsorption of pharmaceutical compounds from aqueous solution using batch and column studies, Chemosphere, 93 (2013) 2076–2085.
[8] R.H. Waring, R.M. Harris, S.C. Mitchell, Plastic contamination of the food chain: a threat to human health?, Maturitas, 115 (2018) 64–68.
[9] E. Bonora, M. Cigolini, DPP-4 inhibitors and cardiovascular disease in type 2 diabetes mellitus. Expectations, observations and perspectives, Nutr. Metab. Cardiovasc. Dis., 26 (2016) 273–284.
[10] B. Gupta, A.K. Gupta, A. Bhatnagar, Treatment of pharmaceutical wastewater using photocatalytic reactor and hybrid system integrated with biofilm based process: mechanistic insights and degradation pathways, J. Environ. Chem. Eng., 11 (2023) 109141, doi: 10.1016/j.jece.2022.109141.
[11] K. Pandya, T.S. Anantha Singh, P. Kodgire, S. Simon, Combined ultrasound cavitation and persulfate for the treatment of pharmaceutical wastewater, Water Sci. Technol., 86 (2022) 2157–2174.
[12] Z. Masood, A. Ikhlaq, O.S. Rizvi, H.A. Aziz, M. Kazmi, F. Qi, A novel hybrid treatment for pharmaceutical wastewater implying electroflocculation, catalytic ozonation with Ni-Co Zeolite 5A° catalyst followed by ceramic membrane filtration, J. Water Process Eng., 51 (2023) 103423, doi: 10.1016/j.jwpe.2022.103423.
[13] Z. Jing, Y. Xu, K. Fan, L. Chun, L. Shaoyan, L. Miaoqi, P. Bo, Performance of advanced treatment of pharmaceutical wastewater by microbubble catalytic ozonation and component variation characteristics of dissolved organic matter, Chin. J. Environ. Eng., 16 (2022) 1469–1479.
[14] R.K. Goswami, K. Agrawal, P. Verma, An exploration of natural synergy using microalgae for the remediation of pharmaceuticals and xenobiotics in wastewater, Algal Res., 64 (2022) 102703, doi: 10.1016/j.algal.2022.102703.
[15] J.K. Samson Ponselvan, A.G. Murugesan, Electrocoagulation of bio-treated pharmaceutical wastewater for RO pretreatment, J. Pharm. Res. Int., 34 (2022) 65–72.
[16] A. Hamdy, M.K. Mostafa, M. Nasr, Zero-valent iron nanoparticles for methylene blue removal from aqueous solutions and textile wastewater treatment, with cost estimation, Water Sci. Technol., 78 (2018) 367–378.
[17] R. Sridar, U. Uma Ramanane, M. Rajasimman, ZnO nanoparticles – synthesis, characterization and its application for phenol removal from synthetic and pharmaceutical industry wastewater, Environ. Nanotechnol. Monit. Manage., 10 (2018) 388–393.
[18] A.S. Mahmoud, M.K. Mostafa, M. Nasr, Regression model, artificial intelligence, and cost estimation for phosphate adsorption using encapsulated nanoscale zero-valent iron, Sep. Sci. Technol., 54 (2019) 13–26.
[19] D.A. Hussein Al-Timimi, Q.F. Alsalhy, A.A. AbdulRazak, Polyethersulfone/amine grafted silica nanoparticles mixed matrix membrane: a comparative study for mebeverine hydrochloride wastewater treatment, Alexandria Eng. J., 66 (2023) 167–190.
[20] I. Fatimah, P.W. Citradewi, G. Purwiandono, H. Hidayat, S. Sagadevan, Nickel oxide decorated reduced graphene oxide synthesized using single bioreductor of *Pometia pinnata* leaves extract as photocatalyst in tetracycline photooxidation and antibacterial agent, Inorg. Chem. Commun., 148 (2023) 110287, doi: 10.1016/j.inoche.2022.110287.
[21] M. Chapalaghi, M. Ahsani, B. Ghofrani, N. Ranjbaran, R. Yegani, A step-by-step assessment of the backwashing process impact on the fouling mitigation of blended PVC/PC and nanocomposite PVC/PC/MAg membranes in a membrane bioreactor (MBR) treating pharmaceutical wastewater, Chem. Eng. Res. Des., 188 (2022) 831–845.
[22] J.S. Afolayan, E. Ajani, S. Saheed, R.D. Folorunsho, M.A. Abdullateef, Green synthesis of copper and silver nanoparticles and their comparative toxicity and antibacterial evaluation in pharmaceutical wastewater treatment, Nanotechnol. Environ. Eng., 8 (2023) 333–346.
[23] T.S. Rajaraman, S.P. Parikh, V.G. Gandhi, Black TiO_2: a review of its properties and conflicting trends, Chem. Eng. J., 389 (2020) 123918, doi: 10.1016/j.cej.2019.123918.
[24] C.G. Aba-Guevara, I.E. Medina-Ramírez, A. Hernández-Ramírez, J. Jáuregui-Rincón, J.A. Lozano-Álvarez, J.L. Rodríguez-López, Comparison of two synthesis methods on the preparation of Fe, N-Co-doped TiO_2 materials for degradation of pharmaceutical compounds under visible light, Ceram. Int., 43 (2017) 5068–5079.
[25] M. Hinojosa-Reyes, R. Camposeco-Solis, F. Ruiz, V. Rodríguez-González, E. Moctezuma, Promotional effect of metal doping on nanostructured TiO_2 during the photocatalytic degradation of 4-chlorophenol and naproxen sodium as pollutants, Mater. Sci. Semicond. Process., 100 (2019) 130–139.
[26] K.S. Varma, R.J. Tayade, K.J. Shah, P.A. Joshi, A.D. Shukla, V.G. Gandhi, Photocatalytic degradation of pharmaceutical and pesticide compounds (PPCs) using doped TiO_2 nanomaterials: a review, Water-Energy Nexus, 3 (2020) 46–61.
[27] K. Oganisian, A. Hreniak, A. Sikora, D. Gaworska-Koniarek, A. Iwan, Synthesis of iron doped titanium dioxide by sol-gel method for magnetic applications, Process. Appl. Ceram., 9 (2015) 43–51.
[28] M.S. Khan, J.A. Shah, N. Riaz, T.A. Butt, A.J. Khan, W. Khalifa, H.H. Gasmi, E.R. Latifee, M. Arshad, A.A. Alawi Al-Naghi, A. Ul-Hamid, M. Arshad, M. Bilal, Synthesis and characterization of Fe-TiO_2 nanomaterial: performance evaluation for RB5 decolorization and in vitro antibacterial studies, Nanomaterials, 11 (2021) 436, doi: 10.3390/nano11020436.
[29] D. Komaraiah, E. Radha, N. Kalarikkal, J. Sivakumar, M.V. Ramana Reddy, R. Sayanna, Structural, optical and

photoluminescence studies of sol-gel synthesized pure and iron doped TiO_2 photocatalysts, Ceram. Int., 45 (2019) 25060–25068.
[30] P.A. Ochoa Rodríguez, G.A. Pecchi, S.G. Casuscelli, V.R. Elías, G.A. Eimer, A simple synthesis way to obtain iron-doped TiO_2 nanoparticles as photocatalytic surfaces, Chem. Phys. Lett., 732 (2019) 136643, doi: 10.1016/j.cplett.2019.136643.
[31] X.Q. Shi, K.Y. Leong, H.Y. Ng, Anaerobic treatment of pharmaceutical wastewater: a critical review, Bioresour. Technol., 245 (2017) 1238–1244.
[32] M.I. Jalees, A. Javed, A. Iqbal, N. Zahara, M. Batool, Comparative isothermal study of phenolic removal from water using different forms of rice husk, Desal. Water Treat., 272 (2022) 220–232.
[33] C. Vatovec, P. Phillips, E. Van Wagoner, T.-M. Scott, E. Furlong, Investigating dynamic sources of pharmaceuticals: demographic and seasonal use are more important than down-the-drain disposal in wastewater effluent in a University City setting, Sci. Total Environ., 572 (2016) 906–914.
[34] S.P. Tripathy, R. Acharya, M. Das, R. Acharya, K. Parida, Adsorptive remediation of Cr(VI) from aqueous solution using cobalt ferrite: kinetics and isotherm studies, Mater. Today Proc., 30 (2020) 289–293.
[35] A. Alshameri, H.P. He, J.X. Zhu, Y.F. Xi, R.L. Zhu, L.Y. Ma, Q. Tao, Adsorption of ammonium by different natural clay minerals: characterization, kinetics and adsorption isotherms, Appl. Clay Sci., 159 (2018) 83–93.
[36] J. Cao, Z.-h. Yang, W.-p. Xiong, Y.-y. Zhou, Y.-r. Peng, X. Li, C.-y. Zhou, R. Xu, Y.-r. Zhang, One-step synthesis of Co-doped UiO-66 nanoparticle with enhanced removal efficiency of tetracycline: simultaneous adsorption and photocatalysis, Chem. Eng. J., 353 (2018) 126–137.
[37] M.I. Jalees, R. Nawaz, Synthesis and application of MoS_2 nanosheets for the removal of amoxicillin from water: response surface method, Arabian J. Sci. Eng., 48 (2023) 443–455.
[38] M.O. Alfred, M.O. Omorogie, O. Bodede, R. Moodley, A. Ogunlaja, O.G. Adeyemi, C. Günter, A. Taubert, I. Iermak, H. Eckert, I.D.A. Silva, A.S.S. de Camargo, A. de Jesus Motheo, S.M. Clarke, E.I. Unuabonah, Solar-active clay-TiO_2 nanocomposites prepared via biomass assisted synthesis: efficient removal of ampicillin, sulfamethoxazole and artemether from water, Chem. Eng. J., 398 (2020) 125544, doi: 10.1016/j.cej.2020.125544.
[39] Y. Cui, X. Deng, Q. Ma, H. Zhang, X. Cheng, X. Li, M. Xie, Q. Cheng, B. Li, Kinetics of photoelectrocatalytic degradation of diclofenac using N, S co-doped TiO_2 nano-crystallite decorated TiO_2 nanotube arrays photoelectrode, Environ. Prot. Eng., 44 (2018) 117–130.
[40] R.P. Cavalcante, R.F. Dantas, B. Bayarri, O. González, J. Giménez, S. Esplugas, A. Machulek Junior, Synthesis and characterization of B-doped TiO_2 and their performance for the degradation of metoprolol, Catal. Today, 252 (2015) 27–34.
[41] V. Tiron, M.A. Ciolan, G. Bulai, G. Mihalache, F.D. Lipsa, R. Jijie, Efficient removal of methylene blue and ciprofloxacin from aqueous solution using flower-like, nanostructured ZnO coating under UV irradiation, Nanomaterials (Basel), 12 (2022) 2193, doi: 10.3390/nano12132193.
[42] K.H. Leong, B.L. Gan, S. Ibrahim, P. Saravanan, Synthesis of surface plasmon resonance (SPR) triggered Ag/TiO_2 photocatalyst for degradation of endocrine disturbing compounds, Appl. Surf. Sci., 319 (2014) 128–135.